

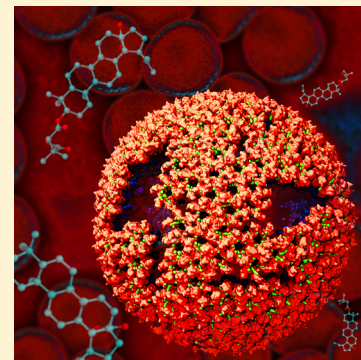
All-Atom Molecular Dynamics of Virus Capsids as Drug Targets

Juan R. Perilla,^{*,†,‡} Jodi A. Hadden,[†] Boon Chong Goh,^{†,‡} Christopher G. Mayne,[†]
and Klaus Schulten^{*,†,‡}

[†]Beckman Institute, and [‡]Department of Physics, University of Illinois at Urbana–Champaign, Urbana, Illinois 61801, United States

Supporting Information

ABSTRACT: Virus capsids are protein shells that package the viral genome. Although their morphology and biological functions can vary markedly, capsids often play critical roles in regulating viral infection pathways. A detailed knowledge of virus capsids, including their dynamic structure, interactions with cellular factors, and the specific roles that they play in the replication cycle, is imperative for the development of antiviral therapeutics. The following Perspective introduces an emerging area of computational biology that focuses on the dynamics of virus capsids and capsid–protein assemblies, with particular emphasis on the effects of small-molecule drug binding on capsid structure, stability, and allosteric pathways. When performed at chemical detail, molecular dynamics simulations can reveal subtle changes in virus capsids induced by drug molecules a fraction of their size. Here, the current challenges of performing all-atom capsid–drug simulations are discussed, along with an outlook on the applicability of virus capsid simulations to reveal novel drug targets.



Viruses represent a serious public health threat, and millions of people die every year from viral diseases. Beyond baseline annual infection rates, periodic outbreaks arising from increased exposure or mutations that enhance transmissibility require emergency action to contain them. In an effort to prevent and combat viral infection, researchers worldwide are endeavoring to develop vaccines and drug-based treatments. Important biological targets for antiviral intervention include viral enzymes, such as the human immunodeficiency virus protease,¹ cellular host factors, which facilitate viral replication, such as cyclophilin-A² and Hsp70 chaperone,³ glycoproteins on the surface of enveloped viruses, such as the neuraminidase of Influenza,⁴ and virus capsids.⁵

Due to their essential structural and functional roles in housing, protecting, and ultimately delivering the viral genome, capsids are of great pharmacological interest as drug targets.

Capsids are specialized protein shells that encase the genetic material of viral pathogens. Due to their essential structural and functional roles in housing, protecting, and ultimately delivering the viral genome, capsids are of great pharmacological interest as drug targets. Assembly, the mechanism by which protein subunits associate to form capsids, can be targeted for disruption either in terms of timing or the geometry of formation, leading to the production of aberrant, nonviable capsids or alternative superstructures that do not suitably encapsulate the genetic material. Improperly formed capsids can interfere significantly with various stages of the viral life

cycle, including RNA reverse transcription and cellular trafficking.⁶ Conversely, disassembly can be targeted by locking the capsid or otherwise disrupting the uncoating process, preventing the release of genetic material and rendering the virus particle noninfective. Disassembly may also be triggered prematurely, such that genetic material is released at an inappropriate time or location. Many small-molecule drug compounds have been developed to inhibit appropriate viral assembly and uncoating, providing a means to thwart completion of both the replication and infection processes.

While vaccines are administered to promote acquired immunity against viruses, antibodies and drug compounds are dispensed primarily as postinfection therapeutics, providing emergency-response treatment and relief to patients. Small-molecule drugs (typically <900 Da) are of particular interest to the chemistry and pharmacology communities because they are less expensive to develop and have commercial potential to be synthesized cheaply and quickly once past clinical trials. Owing to their minimal size, small-molecule drugs can more easily pass through cellular membranes and penetrate into tissues and are, thus, more readily delivered to sites of infection within the body.

Examples of capsid-specific small-molecule drugs include HAP1, active against hepatitis B virus (HBV),⁷ and PF74, active against human immunodeficiency virus type 1 (HIV-1).⁸ Beyond extensive experimental studies aimed at characterizing capsid–drug interactions, computational methods, particularly molecular dynamics (MD) simulations, are emerging as an essential technique to investigate the effects of small-molecule

Received: March 4, 2016

Accepted: April 29, 2016

drugs on capsid structure and dynamics.⁹ MD simulations are beneficial both for application to known capsid–drug systems as well as for drug discovery.^{10–15} For example, recent work on the interaction of V-073 with poliovirus capsid revealed the atomic basis of drug resistance.¹⁶ Notably, the results of the poliovirus work, as well as research presented in the present Perspective applying MD simulations to study drug-bound HBV and HIV-1 capsids, underscore the importance of simulating not isolated capsid proteins but functional assemblies up to the level of complete capsids. Such studies demonstrate the necessity of employing all-atom models, as well as emulating native environmental conditions, to capture the subtle, yet significant effects of small-molecule drugs on dynamic capsid properties. In the present Perspective, the key steps of preparing a capsid–drug simulation are outlined, data describing drug-bound HBV and HIV-1 capsids are presented, and an outlook on the applicability of MD simulations of virus capsids to reveal novel drug targets is offered.

Virus Capsid Morphology. Virus capsids can be composed of one or more types of protein building blocks (protomers), arranged according to well-defined geometric relationships.⁶ These relationships are leveraged both when solving experimental structures and when building full-scale atomic models for study with MD simulations. Capsid morphology can be governed by icosahedral (e.g., HBV, poliovirus) or helical (e.g., Ebola) symmetry rules or may exhibit a conical, polymorphic structure that lacks overall symmetry (e.g., HIV-1).

The capsids of icosahedral viruses comprise 20 identical triangular faces, adjoined by 12 vertices and 30 edges. As such, their structures can be partitioned into n -fold rotational symmetry axes, around which a $360/n$ rotation produces n equivalent views of the polyhedron. The center of each triangular face denotes a three-fold symmetry axis; each vertex, representing the interface of five triangular faces, denotes a five-fold symmetry axis; edges each denote a two-fold (quasi-six-fold) symmetry axis (Figure 1A). The number of constituent protomers and their organization onto the icosahedral lattice is described by a triangulation number, the primary metric by which such capsids are classified.

The key steps of preparing a capsid–drug simulation are outlined, data describing drug-bound HBV and HIV-1 capsids are presented, and an outlook on the applicability of MD simulations of virus capsids to reveal novel drug targets is offered.

Triangulation number T , defined according to Caspar and Klug's mathematical formulation¹⁷

$$T = H^2 + HK + K^2 \quad (1)$$

where H and K are 0 or positive integers, takes on discrete values in the sequence 1, 3, 4, 7, 9, 13, 16, Practically, T corresponds to the possible subdivisions of one-third of the equilateral triangular faces of an icosahedron that produce smaller geometric units of equal dimension. As such, it determines the number of protomers that constitute an asymmetric unit (T), the number required to form a given icosahedral face ($3T$, three asymmetric units related by three-

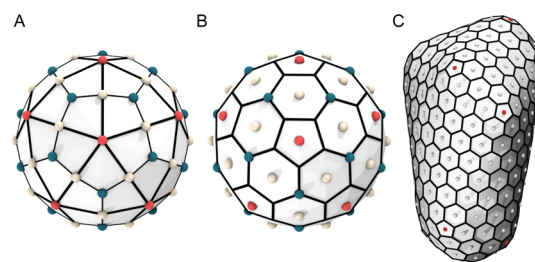


Figure 1. Morphological relationships shared by icosahedral and cone-shaped virus capsids. (A) Schematic illustration of the capsid of an icosahedral virus, delineated according to symmetry operators: three-fold symmetry axes (blue) lie at the center of each triangular face, five-fold symmetry axes (red) lie at each vertex, and two-fold (quasi-six-fold) symmetry axes (beige) lie along each edge. Each kite shape represents an asymmetric unit comprising T protomers. A given icosahedral capsid has three asymmetric units, or $3T$ protomers, per face and is constructed of $60T$ protomers total. (B) Schematic illustration of the capsid of an icosahedral virus, specifically HBV, delineated according to its pentameric (red) and hexameric (beige) capsomeres: pentamers represent an association of five protomers, while hexamers represent an association of six protomers. A given icosahedral capsid contains exactly 12 pentamers, which impart sufficient curvature to close the $60T$ protomer lattice. (C) Schematic illustration of the capsid of a cone-shaped virus, specifically HIV-1, which is similarly constructed of pentamers (red) and hexamers (beige). Although HIV-1 capsids are polymorphic by nature, they nevertheless require (just as icosahedral capsids do) exactly 12 pentamers to achieve lattice closure in their mature form.

fold symmetry), and the number encompassed by the entire capsid assembly ($60T$, twenty $3T$ faces). For example, the HBV capsid, which exists primarily as a $T = 4$ structure, has $3T = 12$ protomers per face and comprises $60T = 240$ total proteins. In many icosahedral viruses, as with HBV, $60T$ copies of a single identical protomer, which occupy quasi-equivalent positions according to their placement along the rotational symmetry axes, make up the full capsid.

Alternative to the asymmetric unit, the protomers of icosahedral capsids can also be grouped into subunits of five or six protomers, centered on five-fold or quasi-six-fold symmetry axes, respectively (Figure 1B). These pentameric and hexameric capsomeres, as they are called, impart unique geometric characteristics to the capsid surface; while associations centered on hexamers lie essentially flat, those centered on pentamers adopt a convex shape. According to Eberhard's theorem,¹⁸ a closed polyhedron, or convex polytope, satisfies the condition

$$3p_3 + 2p_4 + p_5 = 12 + \sum_{k \geq 7} (k - 6) \cdot p_k \quad (2)$$

where p_k indicates the number of k -gonal faces. It follows then that in the absence of triangles (p_3), squares (p_4), and higher-order polygonal faces ($k \geq 7$), a closed capsid requires exactly 12 pentagons and an undetermined number of hexagons. For example, a $T = 4$ capsid, like HBV, is composed of 12 pentamers and 30 hexamers, or 240 protomers. However, virus capsids are not limited to icosahedral symmetries, as conical or coffin-shaped cages also satisfy eq 2. For example, an HIV-1 capsid may contain 216 hexagons and 12 pentagons¹⁹ (Figure 1C), with the latter distributed as five at the apex and seven at the base.

Capsid–Drug Complex Preparation for All-Atom Simulation. Using the geometric relationships and symmetry rules

described above, atomic models of protomer associations up to complete, fully assembled capsids can be constructed for computational study with MD simulations. All-atom structures for elementary subunits, such as asymmetric units or capsomeres, are typically based on experimentally derived coordinates, obtained by either X-ray crystallography or nuclear magnetic resonance (NMR) spectroscopy. In the event that inherently flexible regions of the protomers, particularly loops and chain termini, are not resolved in the experimental structures, these missing features may be modeled based on homology or in silico prediction routines, using software such as Modeler²⁰ or Rosetta.²¹ Complete elementary subunits are assembled into capsids either by applying icosahedral symmetry operations, facilitated by programs like VIPERdb,²² by ordering them onto polyhedral cages with the CageBuilder feature of Chimera,²³ or by fitting them to density maps obtained from cryoelectron microscopy (cryo-EM) or small-angle X-ray scattering (SAXS) experiments with programs such as Situs²⁴ and molecular dynamics flexible fitting (MDFF).²⁵

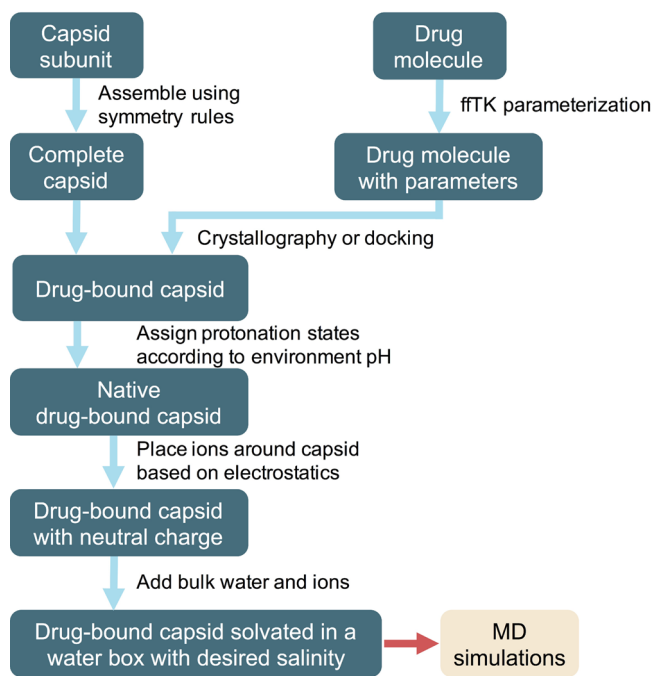
Conical capsids, such as HIV-1, lack overall symmetry, which poses a tremendous challenge to resolving their chemical structure. In these cases, MDFF²⁵ can be essential to obtaining all-atom models. For example, the structure of the helical lattice of HIV-1 (PDB 3J34) was revealed by MDFF, combining the crystal structure of the flat, isolated hexamer,²⁶ the NMR structure of the truncated dimer,²⁷ which provides information regarding the interhexameric contacts, and the cryo-EM-obtained density of cylindrical assemblies containing solely hexamers.¹⁹ On the basis of additional data from cryo-EM and the crystal structure of the hexamer,²⁸ the structure of the entire HIV-1 capsid¹⁹ (PDB 3J3Y), consisting of 12 pentamers and 216 hexamers, was computationally derived by analogy to fullerenes. A key step in the derivation was the construction of a pentamer of hexamers (POH; see Figure 4B) from the experimentally-computationally obtained structure of a hexamer surrounded by six hexamers.¹⁹

Simulating virus capsids in interaction with small-molecule drug compounds involves an extra layer of complexity. First and foremost, an accurate all-atom structure of the whole capsid must be made available to describe drug binding. Second, coordinates and parameters describing the drug and its properties must be obtained. If an experimental structure of the capsid–drug complex is not available, a model structure may be produced by docking the drug molecule into the known binding pocket or interface with programs like AutoDock.²⁹ While the capsid itself can be parametrized readily by application of established biomolecular force fields, compatible parameters dictating the dynamic properties of the nonstandard drug compound must be compiled or otherwise derived ab initio. Fortunately, generalized versions of most popular force fields are available, such as the Charmm General Force Field (CGenFF)³⁰ and the Generalized AMBER Force Field (GAFF),³¹ for the specific purpose of addressing drug-like molecules. Generalized force fields provide parameter coverage for common chemical substructures and functional groups and further define a consistent approach for the development of any additional necessary parameters. Following the stated approach, any parameters not supplied by the generalized force field must be derived in a compatible manner. Specialized tools have been developed to facilitate parametrization, either by analogy to molecules for which parameters are known (e.g., the CGenFF Program^{32,33} and MATCH³⁴) or by computing the parameters

from first-principles (e.g., employing fTK³⁵ and Force Balance³⁶).

Once a complete capsid or capsid–drug complex model is constructed, its environment must be adjusted to mimic native conditions. As many viruses are sensitive to pH, a crucial step of structure preparation involves assignment of appropriate protonation states to polar and charged protein residues. Programs such as propKa³⁷ or H++³⁸ can be used to predict protonation states based on local pK_a values; however, pK_a calculations must be performed on subunits only after they have been assembled into a complete capsid (with drug bound, if applicable) to account for the local pK_a values of all relevant molecular interfaces. Counter ions should then be placed around the capsid system to achieve charge neutrality. The Cionize (short for “Coulombic Ionize”) plugin in VMD³⁹ can be used to compute the Coulomb potential of the capsid system and position cations and anions at suitable points of minimum energy. Deliberate placement of counterions during structure preparation serves to reduce the computational time required for equilibration during the simulation phase of the project. Finally, the capsid system is immersed in a solvent box containing bulk water molecules and sufficient ions to produce the desired salt concentration, typically biological salinity of 150 mM NaCl. A summary of the general workflow for preparing an MD simulation of a small-molecule drug-bound icosahedral virus capsid can be found in Chart 1. To illustrate how

Chart 1. Standard Workflow of Setting up a Simulation of a Drug-Bound Icosahedral Capsid



simulations of capsids and capsid–protein assemblies are currently being used to investigate the dynamic and allosteric effects of small-molecule drug compounds, the following presents data describing drug-bound HBV (Figure 2C) and HIV-1 (Figure 2F) virus capsids.

Drug-Induced Quaternary Rearrangements in the HBV Capsid. HBV is a leading cause of liver disease, cirrhosis, and hepatocellular cancer worldwide. Although a vaccine to prevent viral infection has been available since 1982, there is currently

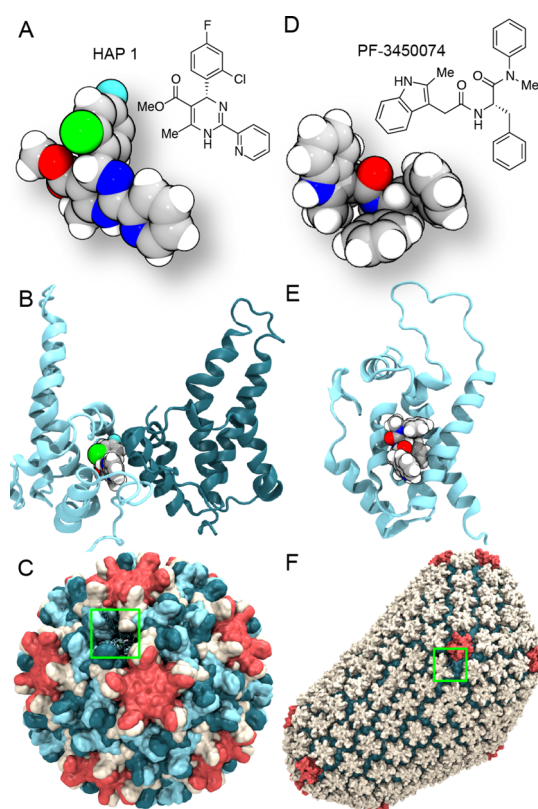


Figure 2. Structures of drug-bound virus capsids. (A) The small-molecule drug HAP1 binds into (B) a closed pocket at the interface between the C (cyan) and D (blue) protomer chains of each asymmetric unit, (C) deep within the surface of the HBV capsid. (D) The small-molecule drug PF74 binds at (E) a surface-exposed interface between the N- and C-terminal domains of adjacent capsid proteins within (F) the pentamers or hexamers of the mature HIV-1 capsid.

no cure for the more than 240 million people the World Health Organization estimates are chronically infected. HBV is found primarily as a $T = 4$ icosahedral structure, whose capsid comprises 120 copies of homodimeric core protein (Cp). Because the HBV capsid plays an essential role in multiple stages of the viral life cycle and the core assembly domain of its Cp constituents has no human homologue that could interfere with drug selectivity *in vivo*,⁴⁰ it represents a promising therapeutic target.

HAP1 (Figure 2A) is a small-molecule drug that affects assembly of the HBV capsid *in vitro*. Particularly, HAP1 enhances capsid assembly kinetics and, at high concentrations, misdirects assembly to produce aberrant, noncapsid particles⁴¹ that manifest as sheets of hexameric capsomeres.⁴² A number of experimental studies have investigated the effects of HAP1 on HBV structure, including cocrystallization of the drug with a preformed capsid.⁷ Comparison of the HAP1-bound capsid structure with an analogous apo-capsid structure⁷ demonstrated that global structural changes are induced by drug binding. Notably, the changes affected quarternary, but not tertiary, structure, as discussed further below.

To study the effects of HAP1 binding on the dynamics of the HBV capsid, MD simulations were employed. HAP1 (Figure 2A) was parametrized using ffTK, as described in the SI (Figure S1). The drug was positioned in the primary binding site of the HAP1-bound capsid crystal structure⁷ (Figure 2B,C) based on previously modeled drug coordinates describing the capsid–

HAP1 interaction⁴³ (unpublished HAP1 coordinates courtesy of A. Zlotnick, Indiana University). The apo-capsid crystal structure⁷ was utilized as a reference state. Simulations totaling 100 ns were performed for both the apo-capsid and HAP1-bound capsids (~6 million atoms). Analysis of the resulting trajectories revealed that the disparity in quarternary structural arrangements between the apo-capsid and HAP1-bound capsid states becomes more pronounced under native environmental conditions.

A predominant feature observed in the HBV capsid crystal structures is the slight protrusion of the five-fold symmetry axes (icosahedral vertices) of the HAP1-bound capsid compared to those of the apo-capsid.⁷ To quantify the degree of protrusion observed in the simulation data, the relative orientation of asymmetric units was measured with respect to the five-fold (φ_{P5}), three-fold (φ_{P3}), and quasi-six-fold (φ_{P6}) symmetry axes (Figure 3A). Comparison of the capsid trajectories confirms the slight increase of φ_{P5} and concomitant decrease of φ_{P3} and φ_{P6} in the HAP1-bound capsid relative to the apo-capsid (Figure 3B), corresponding to enhanced protrusion of the icosahedral vertices and flattening of the curvature along the icosahedral faces and edges (Figure 3C). These adjustments arise structurally from the expansion on average of the five-fold axes away from the capsid center, with simultaneous compression of the three-fold axes toward the center (see the inset in the right panel of Figure 3B).

The quarternary shifts that arise from HAP1 binding lead to a flattening of the hexameric capsomeres and their interfaces. The observation agrees well with the known preference of Cp to aberrantly form sheets of hexamers under high concentrations of HAP1.⁴¹ Further, as the binding of HAP1 has also been shown to trigger dissociation of preformed capsids,⁴² it may be that the HAP1-bound capsid studied here with MD simulation represents a metastable state in the early stages of disassembly.⁷ Ultimately, these data demonstrate that the binding of HAP1 produces global structural changes in the capsid and that these changes may play a role in the antiviral action of HAP1 against complete HBV capsids.

Drug-Induced Shifts in Allosteric Coupling in the HIV-1 Capsid. HIV-1 infection is classified as a global pandemic by the World Health Organization. Treatments are available, but the virus adapts quickly to antiviral drugs, such that new compounds must be developed continuously. The genes of HIV-1, which are packaged within a capsid, must be inserted into the nucleus of the human cell as a key step in the infection cycle; however, in order to reach the interior of the nucleus, the HIV-1 capsid must take advantage of natural host responses and induce cooperation of the cell itself.² Remarkably, some species of monkeys are immune to HIV-1 because their cells disrupt cellular cooperation with the capsid, attacking it instead. Likewise, pharmacological interventions also seek to attack the capsid, either to interfere with the cooperation of cellular machinery or simply to break the capsid apart, ultimately preventing the viral genes from reaching the nucleus. Such interventions, however, require detailed knowledge of the chemical and physical properties of the capsid as a basis for the development of antiviral drugs.²

The HIV-1 capsid, a conical, polymorphic core composed of many copies of a single capsid protomer (CA), plays a fundamental role in multiple stages of the viral replication cycle.² The rich polymorphism that is observed for retroviral cores is induced by conformational changes in the hinge (CA-hinge) between CA's major domains, namely, the N-terminal

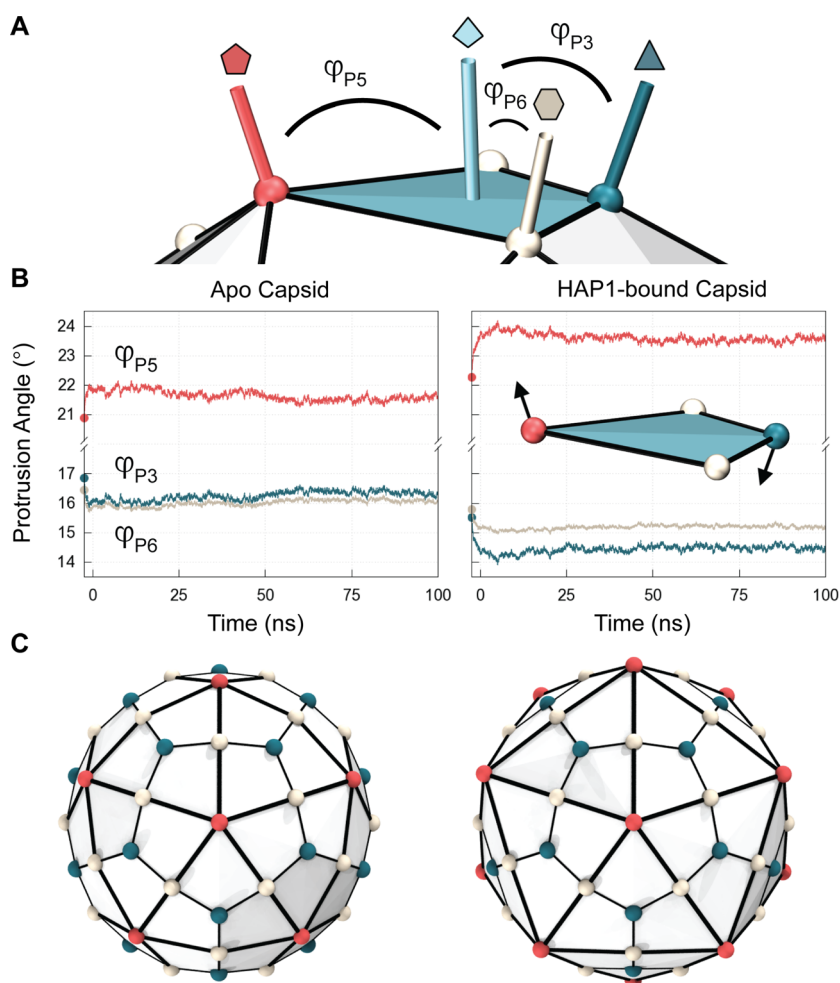


Figure 3. Protrusions of icosahedral symmetry axes in the HBV capsid. (A) Protrusions are measured as the average angle between the plane of the asymmetric unit (cyan) and vectors defined from the center of the capsid through the five-fold (φ_{P5} , red), three-fold (φ_{P3} , blue), and quasi-six-fold (φ_{P6} , beige) symmetry axes, respectively. (B) Comparing the apo-capsid and HAP1-bound capsid structures, φ_{P5} increases while φ_{P3} and φ_{P6} decrease when the drug is present. (C) The geometric adjustments of the asymmetric unit stem primarily from a slight expansion of the five-fold axes away from the capsid center, concomitant with a slight compression of the three-fold axes toward the center (see the inset in the right panel of (B)), causing the icosahedral vertices to protrude and the curvature along the icosahedral faces and edges to flatten. This effect is enhanced 5X for visual clarity.

and C-terminal domains.^{19,46,47} The capsid, upon entering a host cell, during the early stages of infection, mediates a series of interactions with diverse host proteins, engages tubulin for trafficking to the nuclear membrane, and delivers its cargo to the nucleus via the nuclear pore complex.^{2,8,48} After budding from the cell, in the late stages of infection, the mature capsid is assembled from an immature viral particle inside of the HIV-1 virion via an unknown mechanism.^{49,50}

There are multiple drugs known to target the virus capsid during either the early or late stages of the replication cycle, including assembly and maturation inhibitors.⁵¹ Some drugs, such as PF-3450074 (PF74, Figure 2D), target multiple stages of the viral cycle, and the resulting phenotype of PF74-treated viruses involves aberrant assembly, altered nuclear entry pathways, and prevention of uncoating and reverse transcription.⁵² Crystal structures of PF74 bound to monomeric CA,⁵³ as well as to hexameric CA,^{54–56} indicate that the drug binds to the capsid within a pocket at the center of the N-terminal domain (Figure 2E,F). Notably, comparison of crystal structures of apo-form and PF74-bound CA reveals that the structural differences between the two states are extremely

The use of small-molecule drugs to inhibit viral function, along multiple stages of infection, represents a promising avenue for therapeutic intervention; however, successful development of effective drug compounds requires a detailed knowledge of the target protein assembly's structure and dynamic properties, as well as how these properties change upon drug binding.

subtle,⁵² indicating that the mechanism of PF74 antiviral action against the HIV-1 capsid cannot be explained solely in terms of static molecular structure.

Genetic studies were able to identify a set of mutations, called escape mutations, that render HIV-1 resistant to

PF74.^{57,58} Of the five escape mutations incorporated by the PF74-resistant mutants,⁵³ three amino acid substitutions occur near or in the PF74-binding site and directly affect binding affinity.^{52,58} The remaining two mutations occur far from the binding site; in particular, one of the distal mutations is found in the cyclophilin-A binding loop (Figure 4A). Cyclophilin-A (CypA) is an abundant host protein⁵⁹ that binds to the exterior

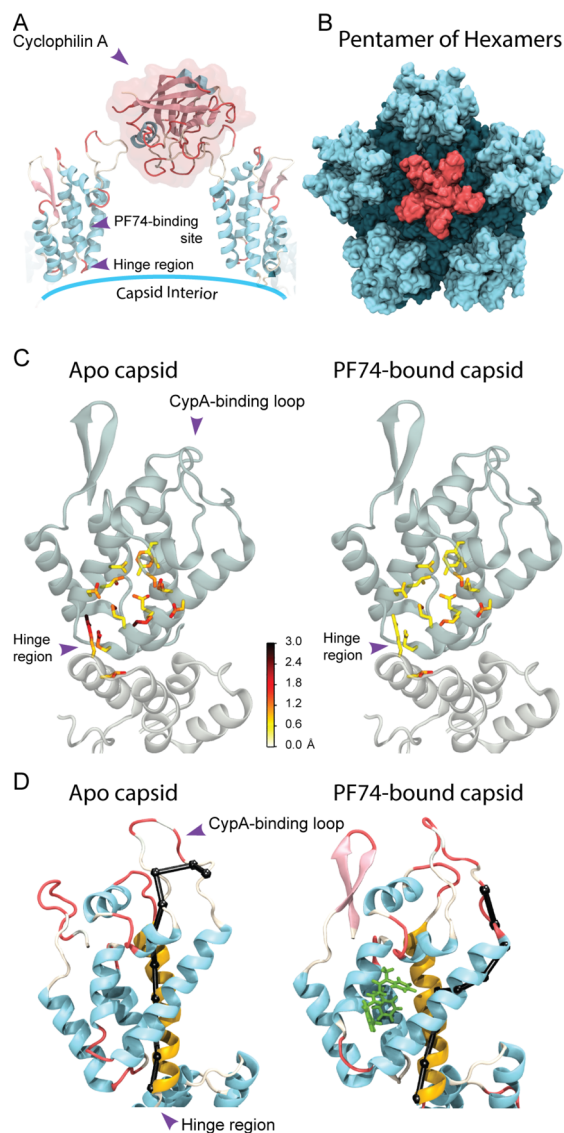


Figure 4. Effect of PF74 on rigidity and dynamics of HIV-1 capsid protein (CA). (A) Interaction between cyclophilin-A (CypA) and the mature HIV-1 capsid is mediated by a binding loop (PDB SFJB).^{44,45} (B) The mature HIV-1 capsid is composed of pentamers and hexamers (Figure 2F). One of its key constituents, a pentamer of hexamers (POH),¹⁹ was simulated in the present study in complex with PF74. (C) Root-mean-square fluctuations (RMSF) of apo-form (left) and PF74-bound (right) CA. Only side chains near the binding site are shown and colored from less (white) to more flexible (red); see the color bar indicating RMSF values). The N-terminal and C-terminal domains of CA are shown in cartoon representation and colored in gray and white, respectively. (D) A highly correlated path (shown in black) of residues connects the CypA binding loop and the hinge region (CA-hinge). In the presence of PF74 (right), a shorter pathway connects the two regions compared to the apo-form of the system (left). Helix seven is colored in yellow for reference.

of the capsid and plays an essential, yet heretofore unknown, role in HIV-1 infection. Interestingly, it has been established that CypA and PF74 interfere with each other, as CypA promotes HIV-1 inhibition by PF74 *in vivo*.⁵⁷ Notably, dynamic coupling between the CypA binding loop and distant residues spread over the CA protein has been detected by both NMR and atomistic MD simulations of complete capsids.^{44,45,60} Such observation of an allosteric effect induced by CypA on the capsid^{44,45} further confirms the absolute necessity to study complete capsids, as well as their interactions with host factors, at atomic-level resolution.

To study the effects of PF74 on the dynamics of the HIV-1 capsid, MD simulations were performed. PF74 (Figure 2D) was parametrized employing ffTK, as described in the SI (Figure S2). Using a previously derived structure of CA with PF74 bound (Figure 2E),¹⁹ the drug was positioned into the binding pocket of both pentameric and hexameric capsomeres, the key building blocks of HIV-1 capsids (typically 186 hexamers and always 12 pentamers), using the available crystal structure for the cross-linked CA-PF74 complex as a template.⁵⁴ A simulation totaling 1.25 μ s was performed for a CA assembly consisting of a pentamer of hexamers (POH) in complex with PF74 (Figure 4B; ~ 1.5 M atoms). A previous simulation of the HIV-1 capsid POH in its apo-form¹⁹ was taken as a reference. Because the atomic interactions between cross-linked and wild-type CA hexamers with PF74 are nearly identical,⁵⁶ the simulation is expected to recapitulate the behavior of wild-type CA. Comparison of the apo-form and PF74-bound simulations immediately suggests a change in dynamics. Indeed, the binding of the drug renders the virus capsid more rigid; although the RMSF of the CA protein backbone are altered only subtly by the binding of PF74, a noticeable decrease in the RMSF of ~ 1 Å was detected for side chains relative to the apo-form (Figure 4C). It has been proposed that such a change in capsid stiffness upon PF74 binding may have important ramifications for infectivity.⁵⁴ Interestingly, CypA binding has also been shown to increase the rigidity of HIV-1 particles.⁴⁵

As mentioned earlier, PF74 escape mutants contain sequence substitutions in regions of CA far from the drug binding site; in particular, one substitution occurs in the CypA binding loop, which has been shown to be dynamically linked with residues spread over the CA protein (including CA-hinge; Figure 4A).⁴⁴ To identify highly correlated paths of residues connecting sites of interest in CA, dynamical network models⁶¹ of the apo-form and PF74-bound POHs were constructed based on MD simulations. Dynamical network analysis is commonly applied to map allosteric pathways in proteins^{61–63} as well as study the effects of ligand binding on such pathways.^{10,64} The network models describing the apo-form and PF74-bound CA systems contain information regarding correlations in all parts of the CA protein, permitting the determination of highly correlated paths of residues that connect any two regions of CA.

The highly correlated path of residues connecting the CypA binding loop and CA-hinge was extracted from the network models created for both apo-form and PF74-bound CA using NetworkView⁶⁵ and projected onto the underlying molecular structure (Figure 4D). Notably, the analysis reveals that for apo-form CA, the CypA binding loop is dynamically linked to the CA-hinge through an α -helix on top of the PF74 binding site (Figure 4D). Conversely, the connection between the CypA binding loop and the CA-hinge occurs through an altered pathway of residues when PF74 is bound (Figure 4D). In addition, the analysis indicates that PF74 induces a stronger

dynamic coupling between these regions, as evidenced by a decrease in average path length by $39.5 \pm 12\%$ (Figure 4D). Along with RMSF demonstrating increased rigidity of CA in the presence of PF74, the results of network analysis suggest that PF74 binding affects the dynamic structure of CA, resulting in altered allosteric pathways within CA assemblies.

Future Challenges. Virus capsids are finely tuned, robust biomolecular devices that play a critical role in the infection of human cells. Disruption of the viral replication cycle by targeting the capsid is not a trivial matter. Although cells have evolved a number of mechanisms to thwart viruses, they fail in many cases. Capsids provide a novel and unexploited therapeutic target for diseases like HIV-1,² where treatments targeting other components of viral structure (such as envelope proteins, polymerases, reverse transcriptases, and integrases) have been exhausted. Hence, the use of small-molecule drugs to inhibit viral function, along multiple stages of infection, represents a promising avenue for therapeutic intervention; however, successful development of effective drug compounds requires a detailed knowledge of the target protein assembly's structure and dynamic properties, as well as how these properties change upon drug binding.

The approach described in this Perspective, focusing on the computational study of virus capsids and capsid–protein assemblies in interaction with known small-molecule drugs, represents an emerging strategy for characterizing the subtle, yet significant effects induced by these compounds. Notably, the described simulations are performed under native environmental conditions and are free of imposed symmetry restraints, allowing them to capture critical shifts in global structure and long-range dynamics. Furthermore, as the relationship between virus capsids and bound drug molecules is ultimately chemical in nature, these simulations emphasize the absolute necessity to investigate such interactions at all-atom detail.

Despite the successful application of MD to the study of virus capsids,⁹ there are still multiple challenges that must be addressed in future work, beyond the context of small-molecule interactions. A key aspect still lacking is the need to account for the presence of RNA in capsids; further, the presence of RNA requires inclusion of appropriate divalent cations, like magnesium (Mg^{2+}), as they are crucial for the structural integrity and biological activity of RNA. In conjunction with RNA structure prediction methods,⁶⁶ pioneering studies applying advanced force fields^{67–71} to the investigation of DNA,^{72–74} ion–protein interactions,⁷⁵ and the HIV-1 capsid in complex with human proteins⁴⁵ will pave the way to modeling capsid–RNA interactions, thus enabling a novel therapeutic target. Furthermore, investigation of the role of pH in capsid assembly and maturation should become accessible to simulation studies through extending recent constant-pH algorithms to larger systems.^{76–81}

Many exciting discoveries regarding virus capsid function and use as drug targets lie just ahead on the horizon, and MD simulations will drive such discoveries pending a series of notable advancements.

In summary, the demonstrated ability of MD simulations to reveal critical insights into the physical and chemical nature of virus capsids marks simulations as an invaluable tool for continued application to study the biology of viruses, as well as strategies for pharmacological interventions going forward. Indeed, many exciting discoveries regarding virus capsid function and use as drug targets lie just ahead on the horizon, and MD simulations will drive such discoveries pending a series of notable advancements, such as developing the ability to predict the structure of viral RNA, the introduction of constant-pH simulations, and the routine parametrization of small-molecule drug compounds.³⁵ Ultimately, biomolecular structure and dynamics, accessible through all-atom MD simulation, hold the key to exploration of novel drug targets that interfere with the viral life cycle through allostery, altered protein–protein interactions, and global structural changes of viral protein assemblies.

■ ASSOCIATED CONTENT

📄 Supporting Information

The Supporting Information is available free of charge on the ACS Publications website at DOI: 10.1021/acs.jpclett.6b00517.

Details regarding parametrization of drug compounds and the simulation setup (PDF)

■ AUTHOR INFORMATION

Corresponding Authors

*E-mail: jperilla@illinois.edu (J.R.P.).

*E-mail: kschulte@ks.uiuc.edu (K.S.).

Notes

The authors declare no competing financial interest.

■ ACKNOWLEDGMENTS

Coordinates for HAP1-bound HBV capsid structure were kindly provided to us by Adam Zlotnick, Indiana University. We acknowledge funding by the National Institutes of Health Grants 9P41GM104601 and R01 GM067887 and the National Science Foundation Grants PHY1430124 and ACI-1524703. This research is part of the Blue Waters sustained-petascale computing project supported by NSF Awards OCI-0725070 and ACI-1238993, the state of Illinois, and the “Computational Microscope” NSF PRAC Award ACI-1440026. An award of computer time was provided by the Innovative and Novel Computational Impact on Theory and Experiment (INCITE) program. This research used resources of the Oak Ridge Leadership Computing Facility at Oak Ridge National Laboratory, which is supported by the Office of Science of the Department of Energy under Contract DE-AC05-00OR22725.

■ REFERENCES

- (1) Torbett, B.; Goodsell, D. S.; Richman, D. *The Future of HIV-1 Therapeutics: Resistance is Futile?* Springer, 2015; Vol. 389.
- (2) Campbell, E. M.; Hope, T. J. HIV-1 Capsid: The Multifaceted Key Player in HIV-1 Infection. *Nat. Rev. Microbiol.* **2015**, *13*, 471–483.
- (3) Taguwa, S.; Maringer, K.; Li, X.; Bernal-Rubio, D.; Rauch, J. N.; Gestwicki, J. E.; Andino, R.; Fernandez-Sesma, A.; Frydman, J. Defining Hsp70 Subnetworks in Dengue Virus Replication Reveals Key Vulnerability in Flavivirus Infection. *Cell* **2015**, *163*, 1108–1123.
- (4) Moscona, A. Neuraminidase Inhibitors for Influenza. *N. Engl. J. Med.* **2005**, *353*, 1363–1373.
- (5) Klumpp, K.; Crépin, T. Capsid Proteins of Enveloped Viruses as Antiviral Drug Targets. *Curr. Opin. Virol.* **2014**, *5*, 63–71.

- (6) Flint, S. J.; Enquist, L. W.; Racaniello, V. R.; Skalka, A. M. *Principles of Virology*, 4th ed.; ASM Press: Washington, DC, 2015.
- (7) Bourne, C. R.; Finn, M. G.; Zlotnick, A. Global Structural Changes in Hepatitis B Capsids Induced by the Assembly Effector HAP1. *J. Virol.* **2006**, *80*, 11055–11061.
- (8) Ambrose, Z.; Aiken, C. HIV-1 Uncoating: Connection to Nuclear Entry and Regulation by Host Proteins. *Virology* **2014**, *454–455*, 371–379.
- (9) Perilla, J. R.; Goh, B. C.; Cassidy, C. K.; Liu, B.; Bernardi, R. C.; Rudack, T.; Yu, H.; Wu, Z.; Schulten, K. Molecular Dynamics Simulations of Large Macromolecular Complexes. *Curr. Opin. Struct. Biol.* **2015**, *31*, 64–74.
- (10) Decherchi, S.; Berteotti, A.; Bottegoni, G.; Rocchia, W.; Cavalli, A. The Ligand Binding Mechanism to Purine Nucleoside Phosphorylase Elucidated via Molecular Dynamics and Machine Learning. *Nat. Commun.* **2015**, *6*, 6155.
- (11) Muddana, H. S.; Fenley, A. T.; Mobley, D. L.; Gilson, M. K. The SAMPL4 Host-Guest Blind Prediction Challenge: an Overview. *J. Comput.-Aided Mol. Des.* **2014**, *28*, 305–317.
- (12) Nichols, S. E.; Swift, R. V.; Amaro, R. E. Rational Prediction with Molecular Dynamics for Hit Identification. *Curr. Top. Med. Chem.* **2012**, *12*, 2002–2012.
- (13) Chen, E.; Swift, R. V.; Alderson, N.; Feher, V. A.; Feng, G.-S.; Amaro, R. E. Computation-Guided Discovery of Influenza Endonuclease Inhibitors. *ACS Med. Chem. Lett.* **2014**, *5*, 61–64.
- (14) Borhani, D. W.; Shaw, D. E. The Future of Molecular Dynamics Simulations in Drug Discovery. *J. Comput.-Aided Mol. Des.* **2012**, *26*, 15–26.
- (15) Durrant, J. D.; McCammon, J. A. Molecular Dynamics Simulations and Drug Discovery. *BMC Biol.* **2011**, *9*, 71.
- (16) Liu, H.-M.; Roberts, J. A.; Moore, D.; Anderson, B.; Pallansch, M. A.; Pevar, D. C.; Collett, M. S.; Oberste, M. S. Characterization of Poliovirus Variants Selected for Resistance to the Antiviral Compound V-073. *Antimicrob. Agents Chemother.* **2012**, *56*, 5568–5574.
- (17) Caspar, D. L. D.; Klug, A. Physical Principles in the Construction of Regular Viruses. *Cold Spring Harbor Symp. Quant. Biol.* **1962**, *27*, 1–24.
- (18) Grünbaum, B. *Convex Polytopes*, Vol. 221 of Graduate Texts in Mathematics; Springer-Verlag: New York, 2003.
- (19) Zhao, G.; Perilla, J. R.; Yufenyuy, E. L.; Meng, X.; Chen, B.; Ning, J.; Ahn, J.; Gronenborn, A. M.; Schulten, K.; Aiken, C.; et al. Mature HIV-1 Capsid Structure by Cryo-Electron Microscopy and All-Atom Molecular Dynamics. *Nature* **2013**, *497*, 643–646.
- (20) Eswar, N.; Webb, B.; Marti-Renom, M. A.; Madhusudhan, M.; Eramian, D.; Shen, M.-y.; Pieper, U.; Sali, A. Comparative Protein Structure Modeling Using MODELLER. *Curr. Protoc. Bioinformatics* **2006**, 5–6.
- (21) Das, R.; Baker, D. Macromolecular Modeling with ROSETTA. *Annu. Rev. Biochem.* **2008**, *77*, 363–382.
- (22) Carrillo-Tripp, M.; Shepherd, C. M.; Borelli, I. A.; Venkataraman, S.; Lander, G.; Natarajan, P.; Johnson, J. E.; Brooks, C. L.; Reddy, V. S. VIPERdb2: An Enhanced and Web API Enabled Relational Database for Structural Virology. *Nucleic Acids Res.* **2009**, *37*, D436–D442.
- (23) Pettersen, E. F.; Goddard, T. D.; Huang, C. C.; Couch, G. S.; Greenblatt, D. M.; Meng, E. C.; Ferrin, T. E. UCSF Chimera - A Visualization System for Exploratory Research and Analysis. *J. Comput. Chem.* **2004**, *25*, 1605–1612.
- (24) Wriggers, W. Using Situs for the Integration of Multi-Resolution Structures. *Biophys. Rev.* **2010**, *2*, 21–27.
- (25) Trabuco, L. G.; Villa, E.; Mitra, K.; Frank, J.; Schulten, K. Flexible Fitting of Atomic Structures into Electron Microscopy Maps Using Molecular Dynamics. *Structure* **2008**, *16*, 673–683.
- (26) Pornillos, O.; Ganser-Pornillos, B. K.; Kelly, B. N.; Hua, Y.; Whitby, F. G.; Stout, C. D.; Sundquist, W. I.; Hill, C. P.; Yeager, M. X-Ray Structures of the Hexameric Building Block of the HIV Capsid. *Cell* **2009**, *137*, 1282–1292.
- (27) Byeon, I.; Meng, X.; Jung, J.; Zhao, G.; Yang, R.; Ahn, J.; Shi, J.; Conzel, J.; Aiken, C.; Zhang, P.; et al. Structural Convergence between CryoEM and NMR Reveals Novel Intersubunit Interactions Critical for HIV-1 Capsid Function. *Cell* **2009**, *139*, 780–790.
- (28) Pornillos, O.; Ganser-Pornillos, B.; Yeager, M. Atomic-Level Modelling of the HIV Capsid. *Nature* **2011**, *469*, 424–427.
- (29) Morris, G. M.; Huey, R.; Lindstrom, W.; Sanner, M. F.; Belew, R. K.; Goodsell, D. S.; Olson, A. J. Autodock4 and AutoDockTools4: Automated Docking with Selective Receptor Flexibility. *J. Comput. Chem.* **2009**, *30*, 2785–2791.
- (30) Vanommeslaeghe, K.; Hatcher, E.; Acharya, C.; Kundu, S.; Zhong, S.; Shim, J.; Darian, E.; Guvench, O.; Lopes, P.; Vorobyov, I.; et al. CHARMM General Force Field: A Force Field for Drug-Like Molecules Compatible with the CHARMM All-Atom Additive Biological Force Fields. *J. Comput. Chem.* **2009**, *31*, 671–690.
- (31) Wang, J.; Wolf, R. M.; Caldwell, J. W.; Kollman, P. A.; Case, D. A. Development and Testing of a General AMBER Force Field. *J. Comput. Chem.* **2004**, *25*, 1157–1174.
- (32) Vanommeslaeghe, K.; MacKerell, A. D., Jr. Automation of the CHARMM General Force Field (CGenFF) I: Bond Perception and Atom Typing. *J. Chem. Inf. Model.* **2012**, *52*, 3144–3154.
- (33) Vanommeslaeghe, K.; Raman, E. P.; MacKerell, A. D., Jr. Automation of the CHARMM General Force Field (CGenFF) II: Assignment of Bonded Parameters and Partial Atomic Charges. *J. Chem. Inf. Model.* **2012**, *52*, 3155–3168.
- (34) Yesselman, J. D.; Price, D. J.; Knight, J. L.; Brooks, C. L., III MATCH: An Atom-Typing Toolset for Molecular Mechanics Force Fields. *J. Comput. Chem.* **2012**, *33*, 189–202.
- (35) Mayne, C. G.; Saam, J.; Schulten, K.; Tajkhorshid, E.; Gumbart, J. C. Rapid Parameterization of Small Molecules Using the Force Field Toolkit. *J. Comput. Chem.* **2013**, *34*, 2757–2770.
- (36) Wang, L.-P.; Chen, J.; Van Voorhis, T. Systematic Parameterization of Polarizable Force Fields from Quantum Chemistry Data. *J. Chem. Theory Comput.* **2013**, *9*, 452–460.
- (37) Sondergaard, C. R.; Olsson, M. H.; Rostkowski, M.; Jensen, J. H. Improved Treatment of Ligands and Coupling Effects in Empirical Calculation and Rationalization of pKa Values. *J. Chem. Theory Comput.* **2011**, *7*, 2284–2295.
- (38) Anandakrishnan, R.; Aguilar, B.; Onufriev, A. V. H++ 3.0: Automating pK Prediction and the Preparation of Biomolecular Structures for Atomistic Molecular Modeling and Simulations. *Nucleic Acids Res.* **2012**, *40*, W537–W541.
- (39) Humphrey, W.; Dalke, A.; Schulten, K. VMD - Visual Molecular Dynamics. *J. Mol. Graphics* **1996**, *14*, 33–38.
- (40) Kanduc, D.; Ricco, R. Hepatitis B Virus and Homo Sapiens Proteome-Wide Analysis: A Profusion of Viral Peptide Overlaps in Neuron-Specific Human Proteins. *Biologics: Targets & Therapy* **2010**, *4*, 75.
- (41) Zlotnick, A.; Mukhopadhyay, S. Virus Assembly, Allostery and Antivirals. *Trends Microbiol.* **2011**, *19*, 14–23.
- (42) Stray, S. J.; Bourne, C. R.; Punna, S.; Lewis, W. G.; Finn, M.; Zlotnick, A. A Heteroaryldihydropyrimidine Activates and Can Misdirect Hepatitis B Virus Capsid Assembly. *Proc. Natl. Acad. Sci. U. S. A.* **2005**, *102*, 8138–8143.
- (43) Bourne, C.; Lee, S.; Venkataiah, B.; Lee, A.; Korba, B.; Finn, M.; Zlotnick, A. Small-Molecule Effectors of Hepatitis B Virus Capsid Assembly Give Insight into Virus Life Cycle. *J. Virol.* **2008**, *82*, 10262–10270.
- (44) Lu, M.; Hou, G.; Zhang, H.; Suiter, C. L.; Ahn, J.; Byeon, I.-J. L.; Perilla, J. R.; Langmead, C. J.; Hung, I.; Gor'kov, P. L.; et al. Dynamic Allostery Governs Cyclophilin A-HIV Capsid Interplay. *Proc. Natl. Acad. Sci. U. S. A.* **2015**, *112*, 14617–14622.
- (45) Liu, C.; Perilla, J. R.; Ning, J.; Lu, M.; Hou, G.; Ramalho, R.; Himes, B. A.; Zhao, G.; Bedwell, G.; Byeon, I.-J.; et al. Cyclophilin A Stabilizes HIV-1 Capsid through a Novel Non-Canonical Binding Site. *Nat. Commun.* **2016**, *7*, 10714.
- (46) Perilla, J. R.; Gronenborn, A. M. Molecular Architecture of the Retroviral Capsid. *Trends Biochem. Sci.* **2016**, *41*, 410.
- (47) Cardone, G.; Purdy, J. G.; Cheng, N.; Craven, R. C.; Steven, A. C. Visualization of a Missing Link in Retrovirus Capsid Assembly. *Nature* **2009**, *457*, 694–8.

- (48) Hilditch, L.; Towers, G. J. A Model for Cofactor Use during HIV-1 Reverse Transcription and Nuclear Entry. *Curr. Opin. Virol.* **2014**, *4*, 32–36.
- (49) Goh, B. C.; Perilla, J. R.; England, M. R.; Heyrana, K. J.; Craven, R. C.; Schulten, K. Atomic Modeling of an Immature Retroviral Lattice using Molecular Dynamics and Mutagenesis. *Structure* **2015**, *23*, 1414–1425.
- (50) Freed, E. O. HIV-1 Assembly, Release and Maturation. *Nat. Rev. Microbiol.* **2015**, *13*, 484.
- (51) Tedbury, P. R.; Freed, E. O. *The Future of HIV-1 Therapeutics*; Springer, 2015; pp 171–201.
- (52) Zhou, J.; Price, A. J.; Halambage, U. D.; James, L. C.; Aiken, C. HIV-1 Resistance to the Capsid-Targeting Inhibitor PF74 Results in Altered Dependence on Host Factors Required for Virus Nuclear Entry. *J. Virol.* **2015**, *89*, 9068–9079.
- (53) Blair, W. S.; Pickford, C.; Irving, S. L.; Brown, D. G.; Anderson, M.; Bazin, R.; Cao, J.; Ciaramella, G.; Isaacson, J.; Jackson, L.; et al. HIV Capsid is a Tractable Target for Small Molecule Therapeutic Intervention. *PLoS Pathog.* **2010**, *6*, e1001220.
- (54) Price, A. J.; Jacques, D. A.; McEwan, W. A.; Fletcher, A. J.; Essig, S.; Chiu, J. W.; Halambage, U. D.; Aiken, C.; James, L. C. Host Cofactors and Pharmacologic Ligands Share an Essential Interface in HIV-1 Capsid that is Lost upon Disassembly. *PLoS Pathog.* **2014**, *10*, e1004459.
- (55) Bhattacharya, A.; Alam, S. L.; Fricke, T.; Zadrozny, K.; Sedzicki, J.; Taylor, A. B.; Demeler, B.; Pornillos, O.; Ganser-Pornillos, B. K.; Diaz-Griffero, F.; et al. Structural Basis of HIV-1 Capsid Recognition by PF74 and CPSF6. *Proc. Natl. Acad. Sci. U. S. A.* **2014**, *111*, 18625–18630.
- (56) Gres, A. T.; Kirby, K. A.; KewalRamani, V. N.; Tanner, J. J.; Pornillos, O.; Sarafianos, S. G. X-ray crystal structures of native HIV-1 capsid protein reveal conformational variability. *Science* **2015**, *349*, 99–103.
- (57) Shi, J.; Zhou, J.; Shah, V. B.; Aiken, C.; Whitby, K. Small-Molecule Inhibition of Human Immunodeficiency Virus Type 1 Infection by Virus Capsid Destabilization. *J. Virol.* **2011**, *85*, 542–549.
- (58) Shi, J.; Zhou, J.; Halambage, U. D.; Shah, V. B.; Burse, M. J.; Wu, H.; Blair, W. S.; Butler, S. L.; Aiken, C. Compensatory Substitutions in the HIV-1 Capsid Reduce the Fitness Cost Associated with Resistance to a Capsid-Targeting Small-Molecule Inhibitor. *J. Virol.* **2015**, *89*, 208–219.
- (59) Nigro, P.; Pompilio, G.; Capogrossi, M. Cyclophilin A: A Key Player for Human Disease. *Cell Death Dis.* **2013**, *4*, e888.
- (60) Han, Y.; Hou, G.; Suiter, C. L.; Ahn, J.; Byeon, I.-J. L.; Lipton, A. S.; Burton, S.; Hung, I.; Gor'kov, P. L.; Gan, Z.; et al. Magic Angle Spinning NMR Reveals Sequence-Dependent Structural Plasticity, Dynamics, and the Spacer Peptide 1 Conformation in HIV-1 Capsid Protein Assemblies. *J. Am. Chem. Soc.* **2013**, *135*, 17793–803.
- (61) Feher, V. A.; Durrant, J. D.; Van Wart, A. T.; Amaro, R. E. Computational Approaches to Mapping Allosteric Pathways. *Curr. Opin. Struct. Biol.* **2014**, *25*, 98–103.
- (62) Sethi, A.; Eargle, J.; Black, A. A.; Luthey-Schulten, Z. Dynamical Networks in tRNA:Protein Complexes. *Proc. Natl. Acad. Sci. U. S. A.* **2009**, *106*, 6620–6625.
- (63) Heyrana, K.; Goh, B. C.; Perilla, J. R.; Nguyen, T.-L. N.; England, M. R.; Bewley, M. C.; Schulten, K.; Craven, R. Charged Residues in Structurally Dynamic Capsid Surface Loops Regulate Rous Sarcoma Virus Assembly. *J. Virol.* **2016**, DOI: 10.1128/JVI.00378-16.
- (64) Guo, J.; Pang, X.; Zhou, H.-X. Two Pathways Mediate Interdomain Allosteric Regulation in Pin1. *Structure* **2015**, *23*, 237–247.
- (65) Eargle, J.; Luthey-Schulten, Z. NetworkView: 3D Display and Analysis of Protein-RNA Interaction Networks. *Bioinformatics* **2012**, *28*, 3000–3001.
- (66) Lorenz, R.; Bernhart, S. H.; Höner zu Siederdisen, C.; Tafer, H.; Flamm, C.; Stadler, P. F.; Hofacker, I. L. ViennaRNA Package 2.0. *Algorithms Mol. Biol.* **2011**, *6*, 26.
- (67) Yin, J.; Fenley, A. T.; Henriksen, N. M.; Gilson, M. K. Toward Improved Force-Field Accuracy through Sensitivity Analysis of Host-Guest Binding Thermodynamics. *J. Phys. Chem. B* **2015**, *119*, 10145–10155.
- (68) Huang, J.; Lopes, P. E.; Roux, B.; MacKerell, A. D., Jr. Recent Advances in Polarizable Force Fields for Macromolecules: Microsecond Simulations of Proteins using the Classical Drude Oscillator Model. *J. Phys. Chem. Lett.* **2014**, *5*, 3144–3150.
- (69) Shi, Y.; Xia, Z.; Zhang, J.; Best, R.; Wu, C.; Ponder, J. W.; Ren, P. Polarizable Atomic Multipole-Based AMOEBA Force Field for Proteins. *J. Chem. Theory Comput.* **2013**, *9*, 4046–4063.
- (70) Cisneros, G. A.; Karttunen, M.; Ren, P.; Sagui, C. Classical Electrostatics for Biomolecular Simulations. *Chem. Rev.* **2014**, *114*, 779–814.
- (71) Wang, L.-P.; Head-Gordon, T.; Ponder, J. W.; Ren, P.; Chodera, J. D.; Eastman, P. K.; Martinez, T. J.; Pande, V. S. Systematic Improvement of a Classical Molecular Model of Water. *J. Phys. Chem. B* **2013**, *117*, 9956–9972.
- (72) Cheatham, T. E.; Case, D. A. Twenty-Five Years of Nucleic Acid Simulations. *Biopolymers* **2013**, *99*, 969–977.
- (73) Savelyev, A.; MacKerell, A. D., Jr. All-Atom Polarizable Force Field for DNA Based on the Classical Drude Oscillator Model. *J. Comput. Chem.* **2014**, *35*, 1219–1239.
- (74) Spöner, J.; Banas, P.; Jurecka, P.; Zgarbová, M.; Kuhrova, P.; Havrila, M.; Krepl, M.; Stadlbauer, P.; Otyepka, M. Molecular Dynamics Simulations of Nucleic Acids. From Tetranucleotides to the Ribosome. *J. Phys. Chem. Lett.* **2014**, *5*, 1771–1782.
- (75) Li, H.; Ngo, V.; Da Silva, M. C.; Salahub, D. R.; Callahan, K.; Roux, B.; Noskov, S. Y. Representation of Ion-Protein Interactions Using the Drude Polarizable Force-Field. *J. Phys. Chem. B* **2015**, *119*, 9401–9416.
- (76) Zeng, X.; Mukhopadhyay, S.; Brooks, C. L., III. Residue-Level Resolution of Alphavirus Envelope Protein Interactions in pH-Dependent Fusion. *Proc. Natl. Acad. Sci. U. S. A.* **2015**, *112*, 2034–2039.
- (77) Goh, G. B.; Hulbert, B. S.; Zhou, H.; Brooks, C. L., III. Constant pH Molecular Dynamics of Proteins in Explicit Solvent with Proton Tautomerism. *Proteins: Struct., Funct., Genet.* **2014**, *82*, 1319–1331.
- (78) McGee, T. D., Jr.; Edwards, J.; Roitberg, A. E. pH-REMD Simulations Indicate that the Catalytic Aspartates of HIV-1 Protease Exist Primarily in a Monoprotonated State. *J. Phys. Chem. B* **2014**, *118*, 12577–12585.
- (79) Swails, J. M.; York, D. M.; Roitberg, A. E. Constant pH Replica Exchange Molecular Dynamics in Explicit Solvent Using Discrete Protonation States: Implementation, Testing, and Validation. *J. Chem. Theory Comput.* **2014**, *10*, 1341–1352.
- (80) Chen, Y.; Roux, B. Constant-pH Hybrid Nonequilibrium Molecular Dynamics-Monte Carlo Simulation Method. *J. Chem. Theory Comput.* **2015**, *11*, 3919–3931.
- (81) Ellis, C. R.; Tsai, C.-C.; Hou, X.; Shen, J. Constant pH Molecular Dynamics Reveals pH-modulated Binding of Two Small-molecule BACE1 Inhibitors. *J. Phys. Chem. Lett.* **2016**, *7*, 944–949.